

Article

Not peer-reviewed version

Analysis of the Possibility of Improving the Performance of Clinch-Riveted Joints by Increasing the Depth of the Rivet Press during the Microalloyed HX340 Steel Sheet Joining Process

Łukasz Boda , [Jacek Mucha](#) ^{*} , [Waldemar Witkowski](#)

Posted Date: 8 January 2024

doi: 10.20944/preprints202401.0485.v1

Keywords: clinch-rivet; HX340 steel joining; interlocking joints



Preprints.org is a free multidiscipline platform providing preprint service that is dedicated to making early versions of research outputs permanently available and citable. Preprints posted at Preprints.org appear in Web of Science, Crossref, Google Scholar, Scilit, Europe PMC.

Copyright: This is an open access article distributed under the Creative Commons Attribution License which permits unrestricted use, distribution, and reproduction in any medium, provided the original work is properly cited.

Article

Analysis of the Possibility of Improving the Performance of Clinch-Riveted Joints by Increasing the Depth of the Rivet Press during the Microalloyed HX340 Steel Sheet Joining Process

Łukasz Boda ¹, Jacek Mucha ^{2,*} and Waldemar Witkowski ³

¹ Doctoral School of the Rzeszow University at Technology, al. Powstancow Warszawy 12, 35-959 Rzeszow, Poland; d413@stud.prz.edu.pl

² Faculty of Mechanical Engineering and Aeronautics, Rzeszow University of Technology, al. Powstancow Warszawy 8, 35-959 Rzeszow, Poland; j_mucha@prz.edu.pl

³ Faculty of Mechanical Engineering and Aeronautics, Rzeszow University of Technology, al. Powstancow Warszawy 8, 35-959 Rzeszow, Poland; wwitkowski@prz.edu.pl

* Correspondence: j_mucha@prz.edu.pl; Tel.: +48 178651636

Abstract: The forming mechanism of clinch joints, for various materials arrangement, using a punch and a rigid die, is well known. The basic technological parameter of the process is the parameter X – the minimal thickness of the embossment. Usually, the lower the X parameter, the greater the joint interlock. This paper presents the possibility of forming a pressed joint for two 1.5 [mm] thick sheets made of HX340 steel. The joint was formed using an additional deformable steel rivet with a hardness of 400HV1. Different values of rivet pressing below the initial surface of the upper sheet were chosen: 0, 0.15, 0.30, 0.45 and 0.60 (in [mm]). The punch positioning accuracy was 0.01 [mm]. For the mentioned rivet pressing distances, forming tests were performed using an “SKB” die with three die depths: 1.45, 1.60 and 1.75 (in [mm]). Observations and measurements of the characteristic geometric dimensions of the interlock were made. Furthermore, the strength of the clinch-riveted joints was analysed. The greater the rivet pressing distance, the larger the interlock parameters. Furthermore, depending on the size of the rivet pressing distance, different failure mechanisms of the lap joint were observed in the tensile shear tests.

Keywords: clinch-rivet; HX340 steel joining; interlocking joints

1. Introduction

Until recently, techniques based on resistance welding, welding, or laser welding were the most common methods of joining car body elements. Due to the fact that these processes generate harmful gaseous compounds and influence mechanically and thermally the material structure of the joined elements, other joining processes have been developed. For some time, the clinching process with an additional rivet and self-piercing riveting has been one of the methods most frequently used than welding [1,2]. The mentioned joining techniques allow to obtain a joint with relatively high stiffness and strength compared to clinch joints (“CL”) [3]. Clinching can be used to join galvanized sheets or sheets with other coatings [4]. The clinching technology can replace resistance welding in some cases [5]. Clinching technology has such great potential that it is constantly being developed [6]. Modifications to this technology are being introduced, and one of them is additional local heating of the materials before joining [7] or welding the bottom of the embossment [8]. Another modification of clinching joining technology is joining sheets with a hole already been made in the lower layer [9]. This method is suitable for joining composites with metals. One of the other methods of connecting without the need to make holes is self-piercing riveting (“SPR”) [10,11]. In the “SPR” joining process, the upper sheet is pierced. Hole-less riveting can be used to join together various

metal materials, including aluminum alloys, but also to join together various construction materials, e.g., various metal compositions [12,13] or titanium alloys [14,15].

When joining using the clinch-riveting method, the continuity of the material of the joined sheets is maintained, and there is no intentional puncture of the joined material layers. As a result of the use of an additional rivet to form the clinch joint, a relatively large increase in the maximum load capacity is achieved [16–19].

The formation of the clinch-rivet joint can be performed using a full deformable steel rivet of various hardness [20]. The authors of work [20] presented the results of research on the influence of different hardnesses of the rivets (350HV1, 400HV1, 420HV1) on the forming force, geometric parameters and the load capacity of the joint for steel sheets.

In the case of selected materials, it is also possible to join them with an additional rivet (without damaging the joined sheets) using a die with a flat surface. In [18], a flat die was used to join aluminum alloy sheets. An analysis of the influence of the blank holder force on the geometric parameters and the load capacity of the joint was presented.

The full rivet can be used to repair clinch joints with damage of the joined sheets in the embossment area [21,22]. A rivet with a hole allows for reducing the energy consumption of the forming process while maintaining a high load capacity of the joint [23]. The paper [23] presents the influence of different diameters of the hole in the rivet on the formation and load capacity of the lap joint of DX51D steel sheets. The lowest forming force was observed for a through hole with a diameter of 2.5 [mm]. The formation of the "CR" joint was done using a rivet made of material of different hardness.

A rivet made of aluminum alloy with a hole can also be used to strengthen a damaged clinch joint [24]. In [25], the authors presented research on joining using a solid rivet and a hole rivet in a two-stage forming process. It is also possible to completely simplify the shape of the die and use a special blank holder in the process of pressing the rivet into the joined materials [26]. Another method of joining using a full rivet was presented in works [27–32]. To join layers of different materials, a high-hardness rivet was used. The rivet punched a hole, and afterward it was blocked with the joined material.

All modifications and innovations in pressure joining technologies are one of the trends in the automotive industry [33,34]. It should be mentioned that each method of joining thin-walled elements causes deformation of the material around the joining point. During joining, there is a local change in the structure of the material and there is a specific deformation of the surface of the joined sheets [35].

This work presents research, results, and analysis of the possibility of using a steel deformable rivet with a hardness of 400HV1 as an additional element for forming a clinch joints for sheets made of micro-alloyed steel and F type zinc coating (ZiNc). A solid full rivet was used to form the clinch-rivet joints. The rivet was pressed to a different depth (offset) relative to the upper surface of the sheets using an 'SKB' die. Forming with different offsets was carried out for three different 'SKB' die depths with movable and fixed segments. In addition, the energy consumption of the forming process was analysed for various variants of the die depth. The basic geometry in the cross-section of the joints was measured, and the deformation of the sheets was measured in the case of the highest observed values of sheet deviation, i.e. for the case of the matrix depth $h_d=1.45$ [mm]. The load capacity of the joints was also tested for a lap joint made of 1.5 [mm] thick HX340 steel sheets.

2. Materials and Methods

2.1. Materials

The micro-alloy steel, produced at the U.S. Steel Košice plant, which is increasingly used for structural elements of car bodies, was used in experimental tests. The thickness of the sheets was 1.5 ± 0.11 [mm] (according to the EN 10143/06 standard [36]), and the material nomenclature was HX340LAD+Z (EN 10346/09 standard [37]) with a ZiNc coating (100 [g/m²]) with an average

thickness of 8 [μm] (according to the EN 10346/09 standard). The basic chemical composition and mechanical properties are presented in Tables 1 and 2.

Table 1. Chemical composition of HX340LAD+Z sheet (maximum percentage by weight [%]).

| Mn | Si | Ti | C | Nb | P | S | Al | Fe |
|------|------|-------|------|-------|------|-------|-------|-----------|
| 0.88 | 0.01 | 0.011 | 0.09 | 0.031 | 0.02 | 0.007 | 0.032 | remainder |

Table 2. Mechanical properties of sheets HX340LAD+Z.

| Material designation | Surface finish +Z [g/m²] | Young’s modulus E, [GPa] | Poisson’s ratio | Yield strength R _{p0.2} [MPa] | Tensile strength R _m , [MPa] | Elongation after fracture A ₈₀ , [%] | Strength coefficient K, [MPa] | Strain hardening exponent n, [-] |
|----------------------|--------------------------|--------------------------|-----------------|--|---|---|-------------------------------|----------------------------------|
| HX340 | zinc layer quality 100 | 188 | 0.29 | 365 | 463 | 29 | 807 | 0.16 |

The deformable steel rivet, type A5x5-2Al, used in the “CR” joining technology had an average hardness of 400HV1. The characteristics of the rivet were presented in [20,23]. The hardness measurement (average of 5 measurements) using the Vickers method was performed using a Matsuzawa micro-hardness tester, type Micro-Sa, Seiki Co, Ltd, at a load of 10 [N] (in accordance with the ISO 6507-1:2018 standard [38]).

2.2. Mechanical joining process

The joints were formed in the Pressed Joints Laboratory of the Machine Design Department at Rzeszow University of Technology. The forming press consisted of a C-shaped frame and an EMPK electric drive system with a maximum pressing force of 100 [kN]. The press measuring system is characterized by a displacement measurement accuracy of 0.01 [mm]. The maximum force measurement error was not greater than 0.5% of the actual pressing force. The joint forming process consisted of feeding the rivet from the clinch riveting punch system and then moving it to the punch bush (Figure 1). The joints were formed using a special rivet punch system with an automatic mechanism to insert the rivet into the space in front of the pressing punch. The rivet was positioned in front of the pressing punch on the appropriate sliders placed in the holes in the bush. Then, the rivet was gradually pressed into the joined sheets. After the bottom sheet came into contact with the bottom of the die, due to the pressure of the punch on the rivet, the rivet material flowed more intensively in the radial direction. The rivet and sheet material filled the space of the movable segments of the die. After the face of the rivet pressing punch reached a predetermined position, the punch system was withdrawn and the joint was formed. The position of the rivet was controlled with an accuracy of 0.01 [mm].

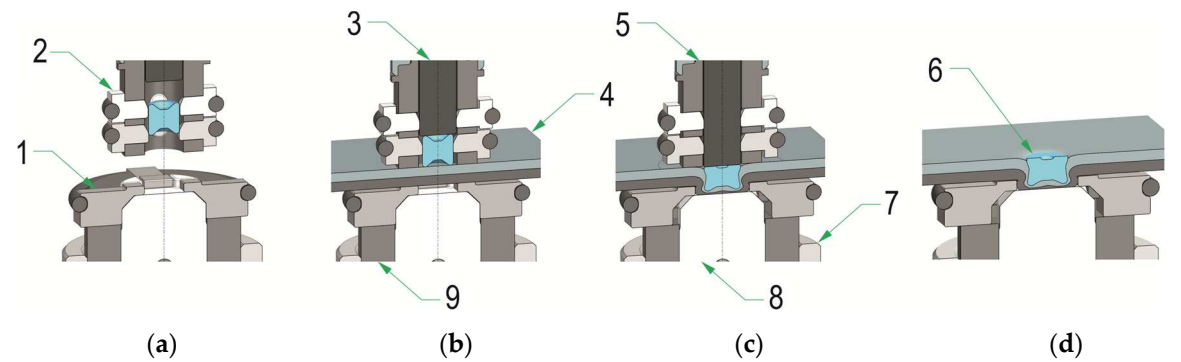


Figure 1. The main phases of the sheet joining process: a) the rivet positioning in the clinch riveting punch system before placing the sheets for joining - phase I, b) pressing the rivet into the joined layers of materials - phase II, c) final pressing of the rivet at the bottom of the die - phase III, d) clinch-rivet joint after retraction of the clinch riveting punch system; 1-SKB die with movable segments, 2-sliders in the punch system, 3-punch, 4-joined sheets, 5-bush of the punch system, 6-rivet after forming process, 7-bush of the die system, 8-pin of the die system, 9- bush die with movable segments.

For research on the formation of “CR” joints for two HX340 steel sheets, a die with 3 depths $h_d=1.45, 1.60, 1.75$ (in [mm]) and a flat bottom was used (Figure 2). Forming was carried out using a clinch rivet punch system (Figure 2a) and a developed replaceable die system (Figure 2b, c) allowing easy replacement in the bush holder (Figure 2c) and mounting on the press stand. The characteristic shape and dimensions of the rivet, punch, and dies are shown in Figure 3. First, basic joints were made for the upper surface of the rivet to obtain a position corresponding to the initial position of the upper surface of the sheets. Then, for each depth of the die, a clinch-rivet joints were formed for additional 4 offset values $o_f=0.15, 0.30, 0.45, 0.60$ (in [mm]) - Figure 4a. An example of a joint with a rivet offset of the rivet $o_f=0.6$ [mm] is presented in Figure 4b. All tested variants of the “CR” joint are listed in Table 3.

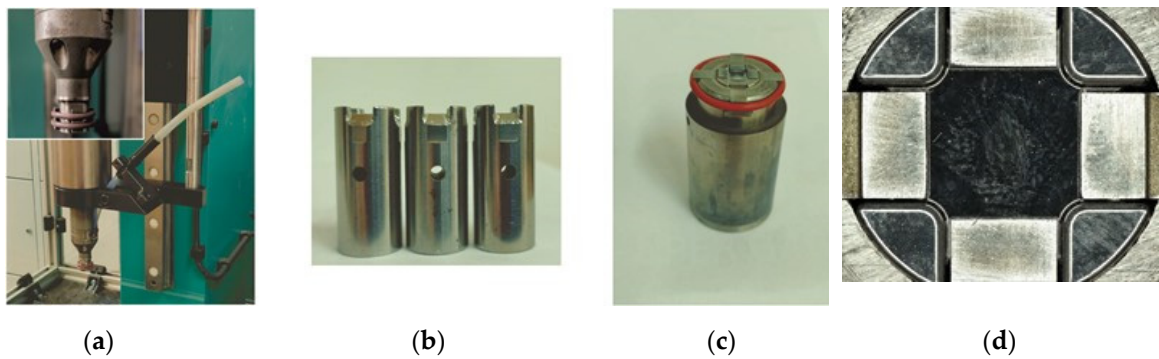


Figure 2. The set of tools used for the experimental formation of “CR” joints: a) the clinch riveting punch system, b) set of pins with a depth of $h_d=1.45$ [mm], 1.60 [mm], 1.75 [mm], c) bush die with pin and movable segments, d) top view of die with flat bottom.

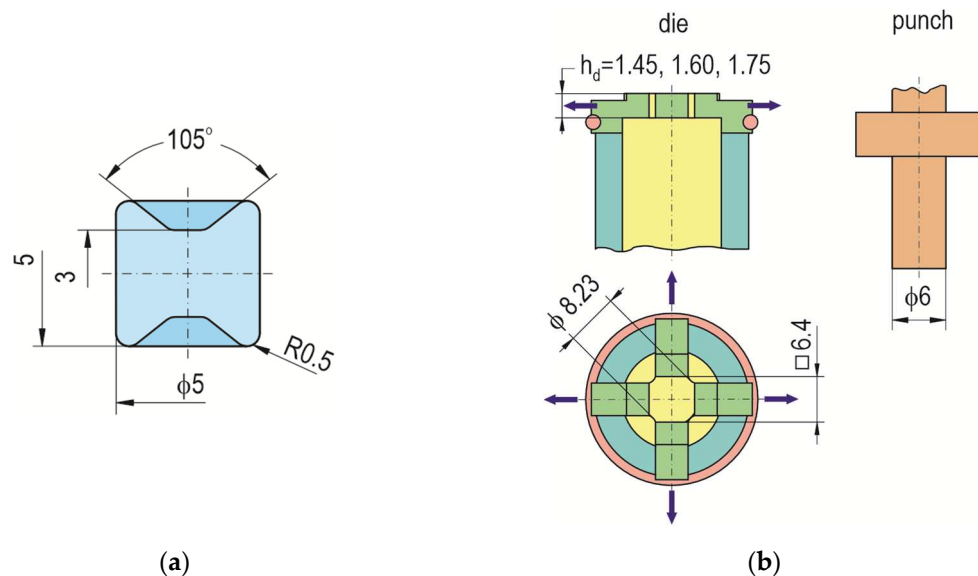


Figure 3. The basic geometry and dimension of: a) the rivets, b) the die and rivet pressing punch (in [mm]).

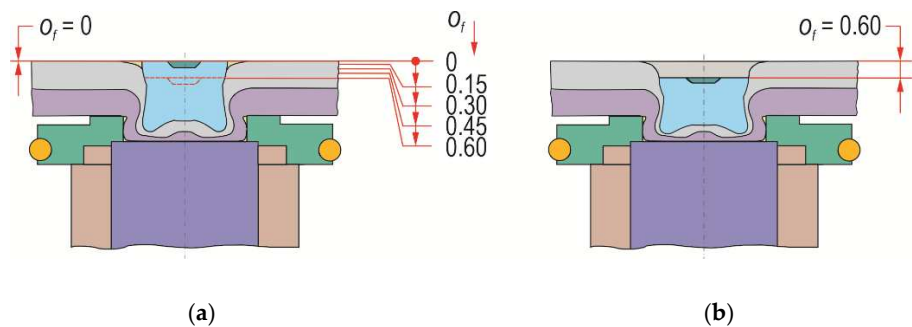


Figure 4. The relative position of the upper surface of the rivet in the joint: a) rivet final position for offset $o_f=0$, b) rivet final position for offset $o_f=0.6$ (o_f in [mm]).

Table 3. The list of “CR” joint variants.

| Offset dimension o_f [mm] | Die depth h_d [mm] | | |
|-----------------------------|----------------------|-------|--------|
| | 1.45 | 1.60 | 1.75 |
| 0 | I-00 | II-00 | III-00 |
| 0.15 | I-15 | II-15 | III-15 |
| 0.30 | I-30 | II-30 | III-30 |
| 0.45 | I-45 | II-45 | III-45 |
| 0.60 | I-60 | II-60 | III-60 |

The joint cross-sections were prepared. It was observed that the greatest deviation of the sheets occurred for the case of the die depth $h_d=1.45$ [mm]. The cross-section of the joints was made in the joint axis so that the cross-sectional plane intersected the material flowed between the fixed segments of the die (Figure 5b). Therefore, joint samples were again made according to the diagram in Figure 5a and it was decided to scan the external surfaces of the sheets. The surface of the bottom of the die "3" (Figure 5b) corresponded to the surface "5" of the embossment of the nominal CAD model (Figure 5a). On the basis of the location of the external surfaces of the sheets of the nominal CAD model, the base reference planes were determined to analyse the deviation of the external surfaces of the joint samples. The initial surface of the sheets was measured and on this basis the nominal model of the sheets was established and the base (initial) system of the reference surface was determined (Figure 6a). After the base surfaces of the sheets and the nominal location of the rivet face and the die bottom surfaces were applied, a nominal CAD comparative model was obtained. After measuring on a 3D scanner, a model of the deformed sample was obtained. Then, both models were compared with a common coordinate system (Figure 6b).

The surface deviations of the sheet metal were measured using an ATOS Capsule 200 MV200 scanner. The measurement system was determined by parameters obtained with the acceptance test according to guideline VDI/VDE 2345 Part 3 [39], in line with the GOM Acceptance Test. The measurement system was characterized by the maximum measurement error: sphere spacing error 0.008 [mm] and length measurement error: 0.009 [mm]. After the scan, points along the path were set, and deviations were visualized in the form of an area distribution.

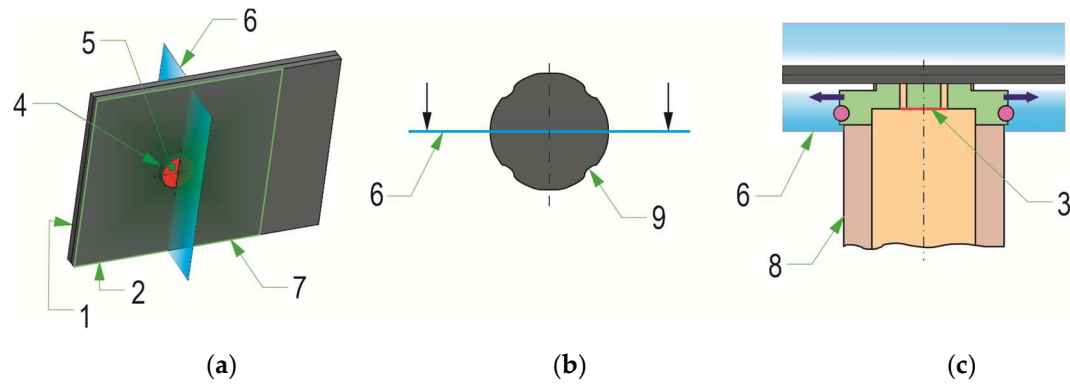


Figure 5. The characteristics of: a) the base external surface of the lower sheet, b) the transverse plane of the joint cross-section, c) the initial position of the sheets in relation to the bottom of the die; 1-upper sheet metal, 2-lower sheet metal, 3-surface of the bottom of the die (reference surface for the position of the sheets), 4-embossment, 5-outer lower surface of the embossment, 6-cross-sectional plane of the joint, 7-boundaries of the scanned area of the upper and lower surfaces of the joint, 8-die with movable segments, 9-places of interaction of fixed segments of the die.

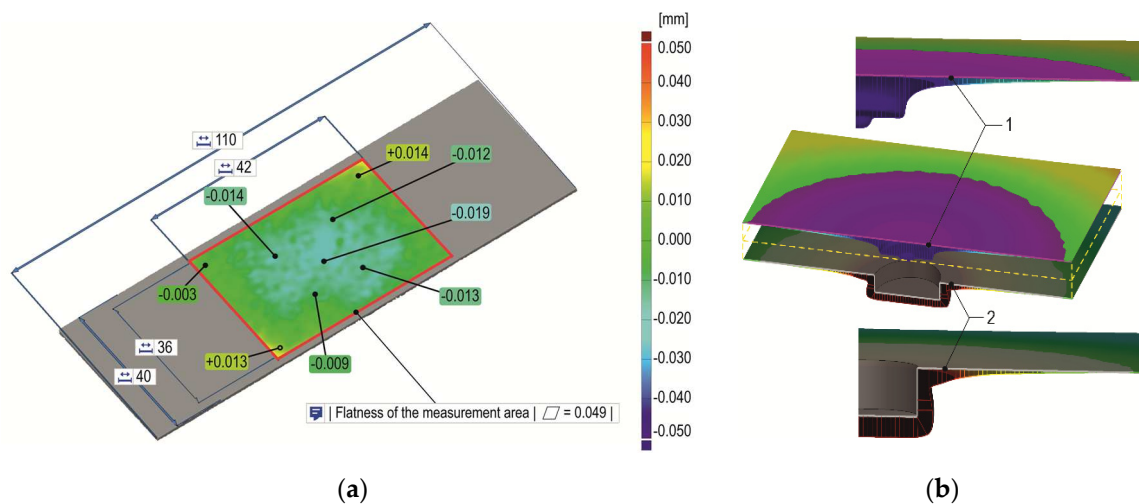


Figure 6. The characteristics of: a) the flatness of the base surface of the sheets, before joining (in [mm]), b) comparison of the 3D scan model with the base model of the location of the characteristic joint surfaces (1-upper base surface, 2-bottom base surface).

For all variants of the joints (Table 3), observations and measurements of characteristic parameters of the joints interlocks were made (Figure 7). Macro photos and joint geometry measurements were made using the VHX7000 optical microscope. The microscope was equipped with a VH-Z20R/Z20T zoom lens. The resolution of a single image was 2048×1536 [px] and the distance between the pixels of the recorded image, in both directions of the XY plane, was 0.0015 [mm].

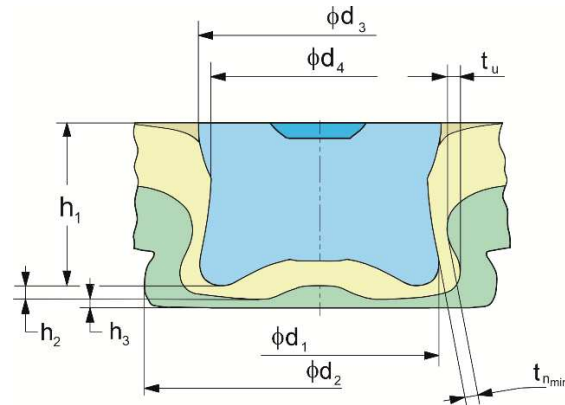


Figure 7. The basic interlock parameters of the “CR” joint.

To analyse the load capacity of the clinch-rivet joints, samples of lap joints, made of sheets with dimensions of 40x110 [mm], were used. The geometry of the lap joint is shown in Figure 8a. The dimensions were determined based on the guidelines given in the ISO 12996: 2013 standard [40]. For each arrangement of lap joints (according to Table 3), seven samples were made. The strength tests of the lap joints were carried out on a tensile test machine with a measuring system of 100 [kN] (Figure 8b).

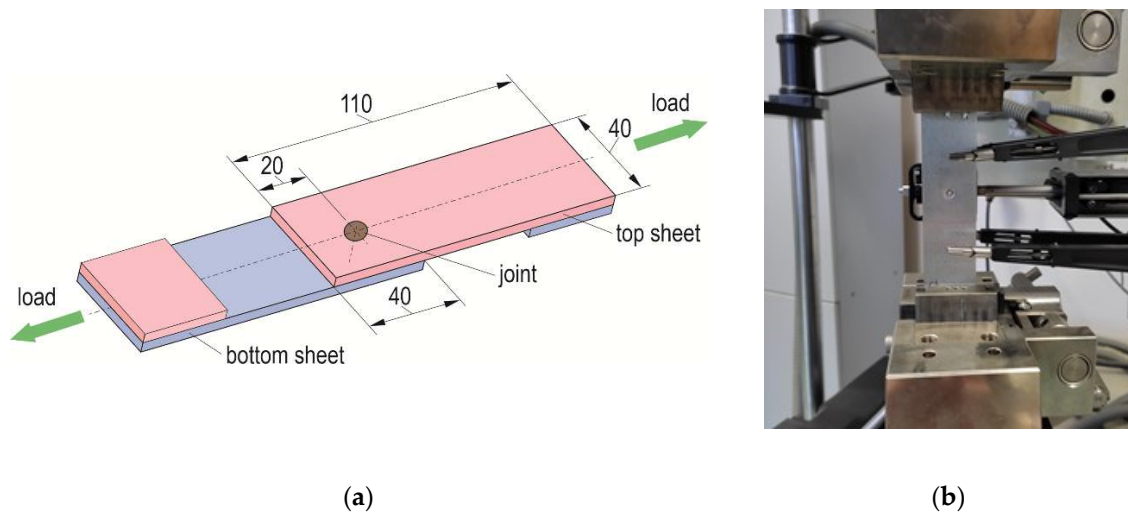


Figure 8. The “CR” joint lap samples: a) dimensions (in [mm]), b) mounted on the tensile test machine with an extensometer system.

3. Results and Discussion

3.1. Joint forming process and interlock parameters

The formation of the “CR” joint using a die with a depth of $h_d=1.45$ [mm] and an offset $o_f=0$ [mm] resulted in the highest forming force required (Figure 9). For the remaining two die depths, a lower forming force was obtained, and for $h_d=1.75$ [mm] the lowest. In each case of the depth of the die, increasing the offset value resulted in an increase in the forming force (Figure 10a). For the case of offset 0 [mm], the impact of the depth of the die was relatively large. Increasing the depth of the die from 1.45 [mm] to 1.75 [mm] (by nearly 20%) resulted in a 12% reduction in the forming force. In addition to changing the depth of the die, the energy consumption of the “CR” joining process can be reduced by using a modified rivet [23].

The smallest influence of the die depth on the forming force was observed for the largest offset $o_f=0.6$ [mm]. The higher value of the offset o_f increases the force loading of the tools. The loads of the tools influence their deformation and wear [41,42]. The highest energy consumption of the forming process was observed for the case $o_f=0.6$ [mm] (Figure 10b). However, the greatest reduction in forming energy consumption was obtained for the case $o_f=0.15$ [mm] and the increase in the depth of the die from $h_d=1.45$ [mm] to 1.75 [mm].

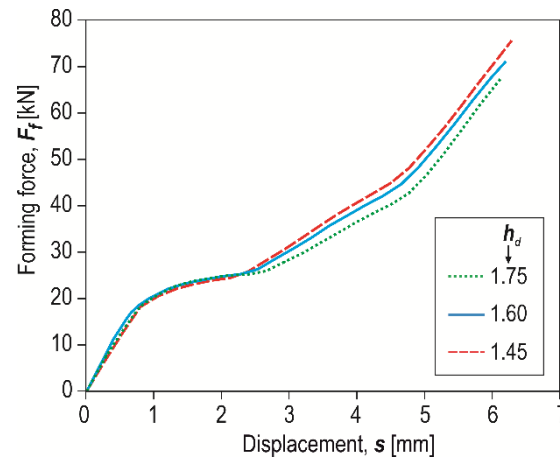


Figure 9. The examples of forming force-displacement diagrams for “CR” joining with the die with three values of the depth (h_d in [mm]).

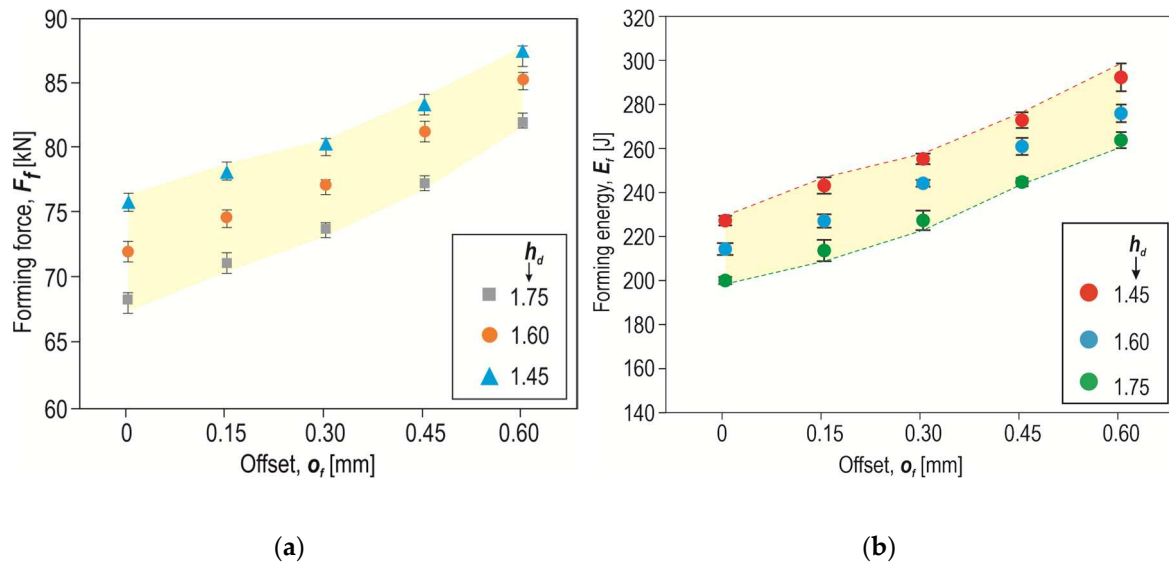


Figure 10. The influence of the offset value o_f on: a) the forming force F_f , b) forming energy consumption E_f (h_d in [mm]).

In the Figure 11 the embossment of the material pressed into the die groove was presented. In all the cases of h_d values, the largest outer diameter of the embossment was obtained for the largest offset (Figure 11). The largest difference in maximum diameter of the embossment between offset 0 [mm] and 0.6 [mm] was observed for the case of forming the joint with a die with $h_d=1.45$ [mm]. The smaller the die depth, the more the fixed die segments influenced the material so that it flowed more intensively, moving the movable segments. The larger the diameter d_2 , the more intensively the sheet material was pressed between the fixed segments. For the offset $o_f=0$ [mm], the differences were insignificant. The more the offset was increased, the greater the differences. Hence, the pictures show changes in the structure and shape of the joint in cross-sections (Figure 12). It is possible to reduce embossment height by joining with an additional rivet (without damaging the joined sheets) when

using a flat die [18]. In [18] it was shown that the higher the pressing force of the sheets, the greater the geometric parameters and load capacity of the joint. A solid and non-deformable rivet (of high hardness) was used in their research.

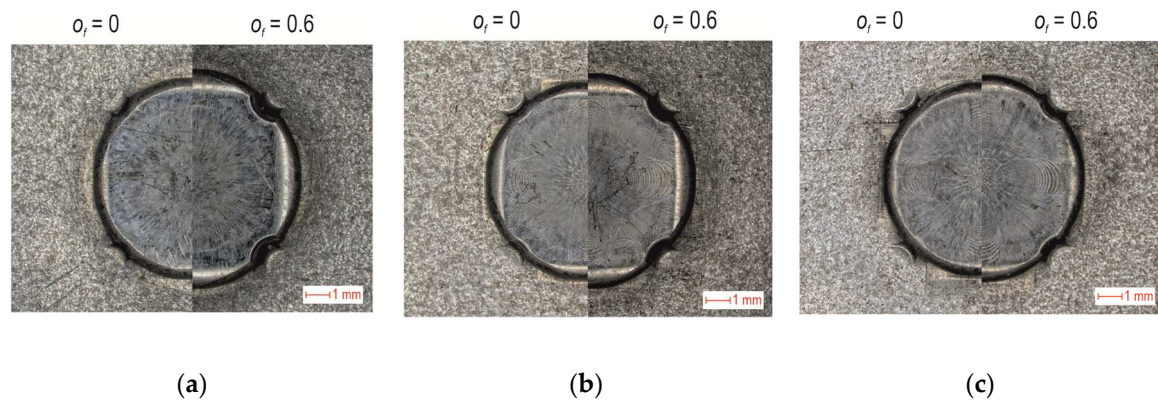


Figure 11. The view of the embossment form the die side of the “CR” joint and the depth of the die: a) $h_d = 1.45$, b) $h_d = 1.60$, c) $h_d = 1.75$ (in [mm]).

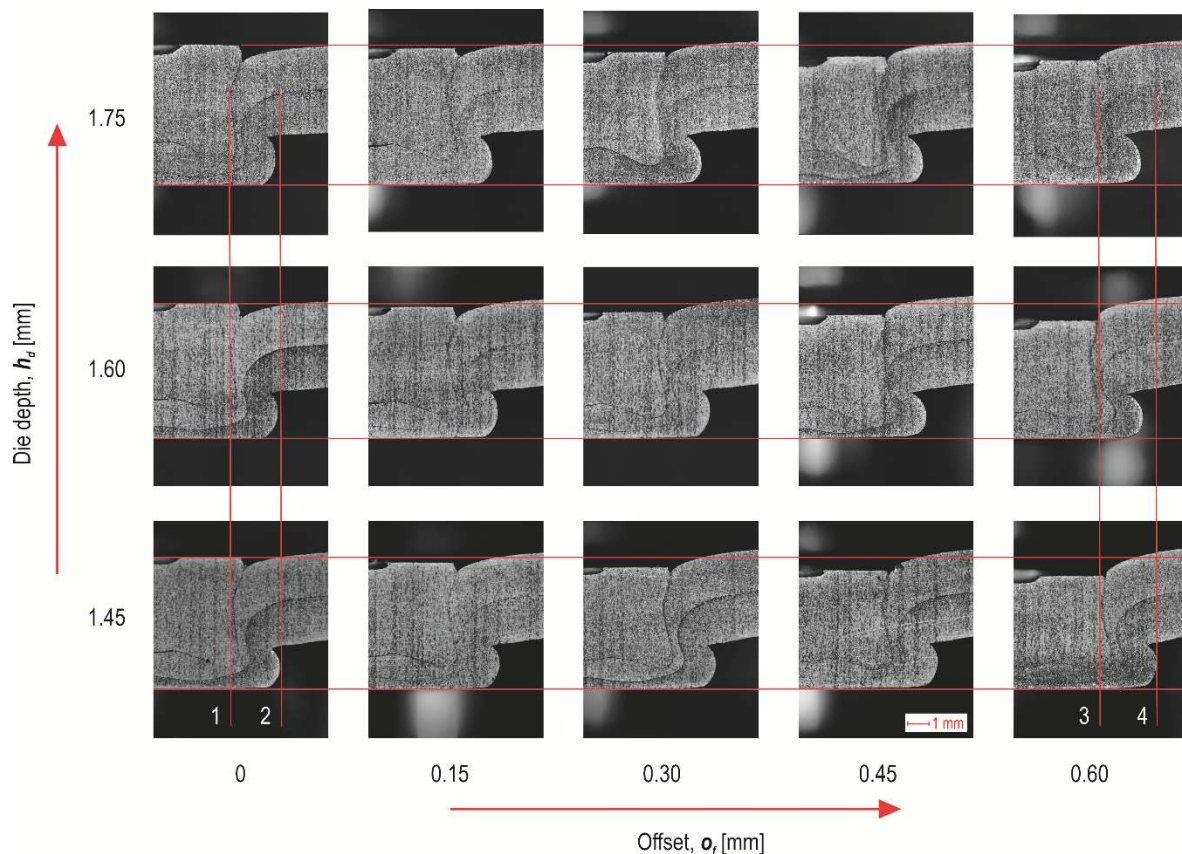


Figure 12. The “CR” joint cross-sections on macro scale (in [mm]).

The higher the offset value, the greater the intensity of the sheet material flow and thus the greater the maximum diameter d_1 of the rivet in the joint (Figure 13a). The greatest impact of the depth of the die on the diameter d_1 was obtained for the largest offset of 0.6 [mm]. The highest minimum thickness of the lower sheet in the interlock (h_3) was for the case of forming a joint with a die with a depth of $h_d = 1.45$ [mm] - Figure 13b. Increasing the depth of the die from 1.45 [mm] to 1.75 [mm] caused the dependence in the minimum thickness of the lower sheet change for an offset greater than 0.45 [mm]. In the case of h_3 thickness, the larger the offset used, the lower the value of this

parameter was obtained. The decrease in this value (h_3) was not the same as for the thickness parameter h_2 . In the case of h_2 , the decrease in value as the offset increased was not as in the case of h_3 . Despite the decrease in the value of h_3 as the offset increased, an increase in the value of the parameter h_2 parameter was observed at an offset greater than 0.45 [mm]. It should be mentioned that in none of the cases analysed a puncture of the two joined layers of sheet metal occurred.

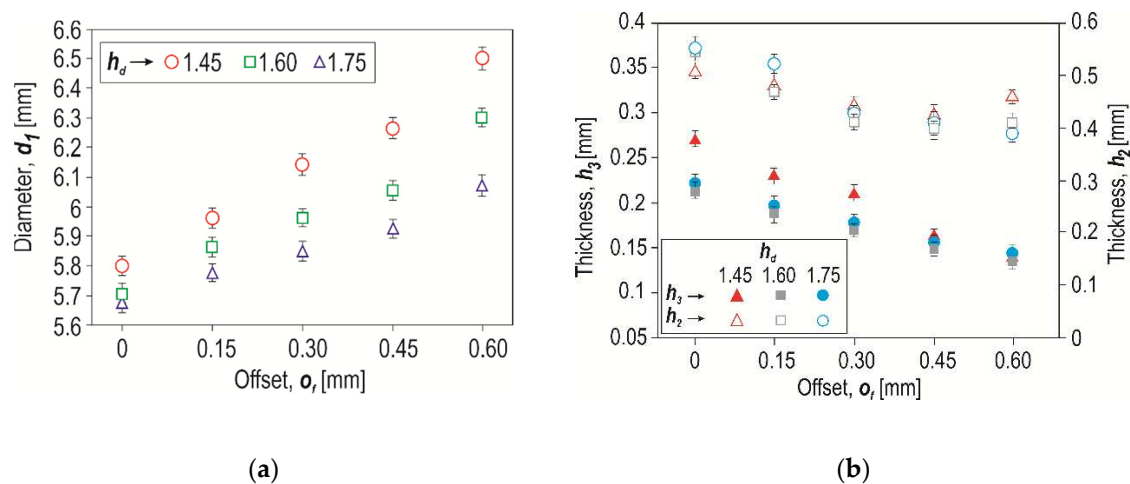


Figure 13. The influence of the depth of the die (h_d) and the offset value (o_f) on: a) the maximum diameter of the rivet – d_1 , b) the minimum thickness of the sheet in the interlock – h_2 and h_3 .

It was also noticed that the offset value significantly influenced the values of the interlock parameters t_u and t_n . When joining high-strength steels, it is not always possible to form an interlock, even with the use of the SPR or clinching method [43,44]. Therefore, the authors of this publication investigate the influence of the change in the depth of insertion of the rivet ($o_f=0-0.6$ [mm]) and the depth of the die ($h_d=1.45-1.75$ [mm]) on the formation of the interlock. For all three depths of the die ($h_d=1.45, 1.60$ and 1.75 [mm]), it was observed that at an offset of 0.15 [mm] there are characteristic values of the interlock parameter t_u (Figure 14a). For an offset greater than 0.15 [mm], there was a significant increase in the parameter t_u . In each case of the die depth, an increase in the interlock parameter t_u was obtained from the offset value of 0.15. The greatest difference in the impact of the depth of the die on the interlock parameter t_u occurred for the offset of 0.6 [mm]. In the case of a minimal thickness of the interlock t_n , the greatest impact of the parameter h_d occurred for an offset of 0 [mm] (Figure 14b). In the range of offset values from 0.15 [mm] to 0.45 [mm], both t_u and t_n increased (for all depths of the die). Increasing the offset value from 0.45 [mm] to 0.6 [mm] resulted in an increase in the parameter t_u and a decrease in the parameter t_n . This happened because the rivet bent the material of the lower sheet so that the size of the interlock increased and the sheet metal thinning in the range of 0.15 [mm] to 0.45 [mm] decreased. Thus, the parameter t_n increased. Only at offset $o_f=0.6$ [mm] the rivet deformation caused thinning of the interlock, so that the value t_n decreased (for all cases of the depth of the die). The use of a rivet with a higher hardness can increase the interlock parameters and increase the load capacity of the clinch-rivet joint [20].

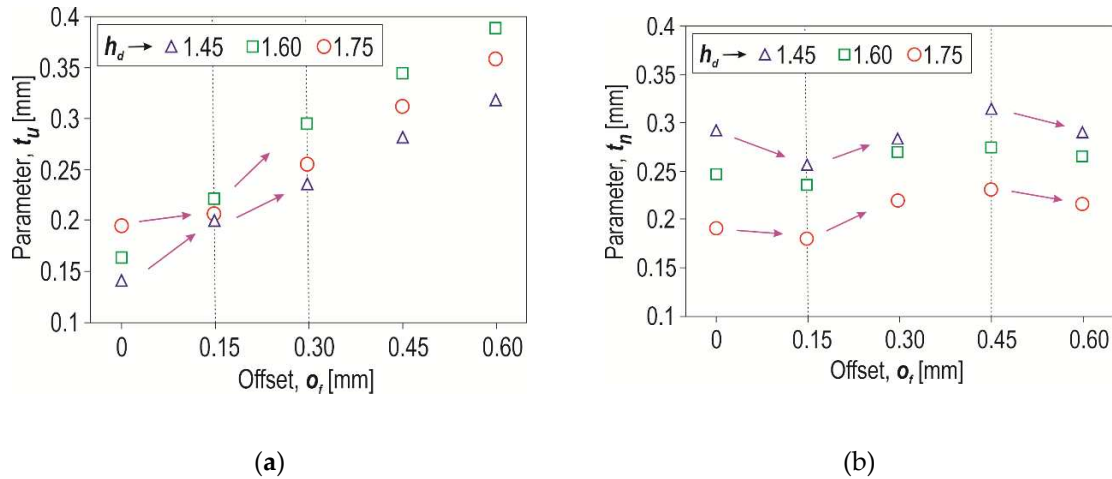


Figure 14. The influence of the depth of the die (h_d) and the offset value (o_f) on the interlock parameters: a) t_u , b) t_n .

3.2. Rivet and sheet deviations

An additional deformable element in the form of a solid rivet indirectly forms an interlock between the joined sheets. To characterize the influence of the offset value and the depth of the die on the deformation of the rivet, its interlock outlines were compared (Figure 15a). Proportionally to the deformation of the rivet, a common internal line of two sheets was formed (Figure 15b). To properly form the sheet interlock, the rivet must fill the space in the die cavity. The highest radial flow of the rivet material was observed for the case of die $h_d=1.45$ [mm] and the maximum offset ($o_f=0.6$ [mm]). In this case, the rivet is most compressed so its material flows in the radial direction (Figure 15a). It was noticed that for this case of (joint formed with a depth of the die $h_d=1.45$ [mm]) the greatest deviation of the sheet surfaces around the joint occurred (Figure 12). Therefore, it was decided to measure and analyse the deformation of the upper and lower sheets. Figure 16 shows the results of the deviations of the upper and lower surfaces of the joined sheets from the base surfaces of the sheets (before joining).

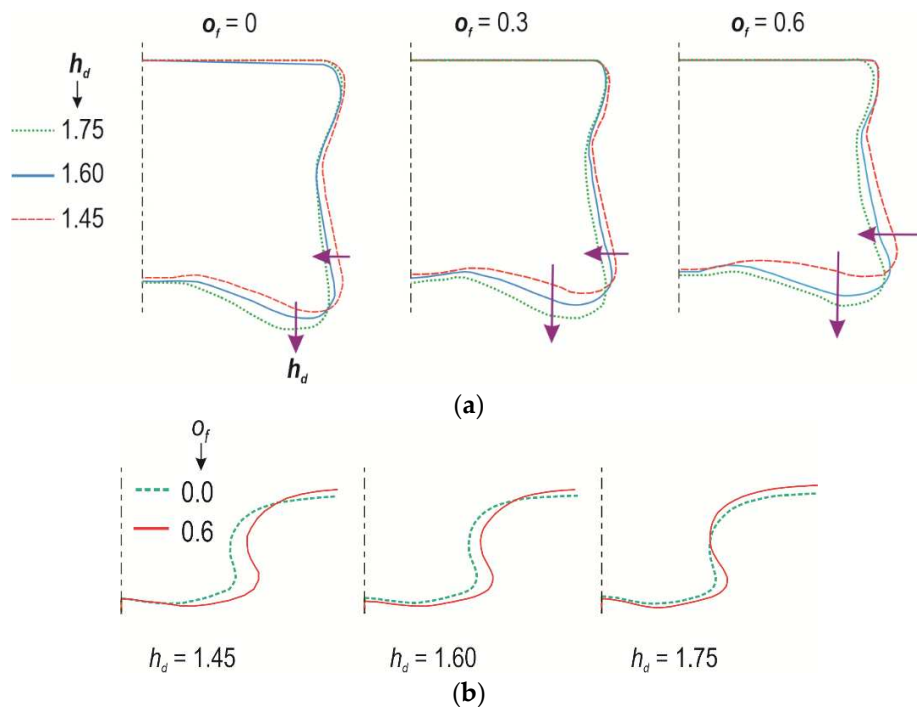


Figure 15. The comparison of the interlock shape for different values of the depth of the die (h_d) and the offset value (o_f): a) for rivet, b) line between lower and upper sheets.

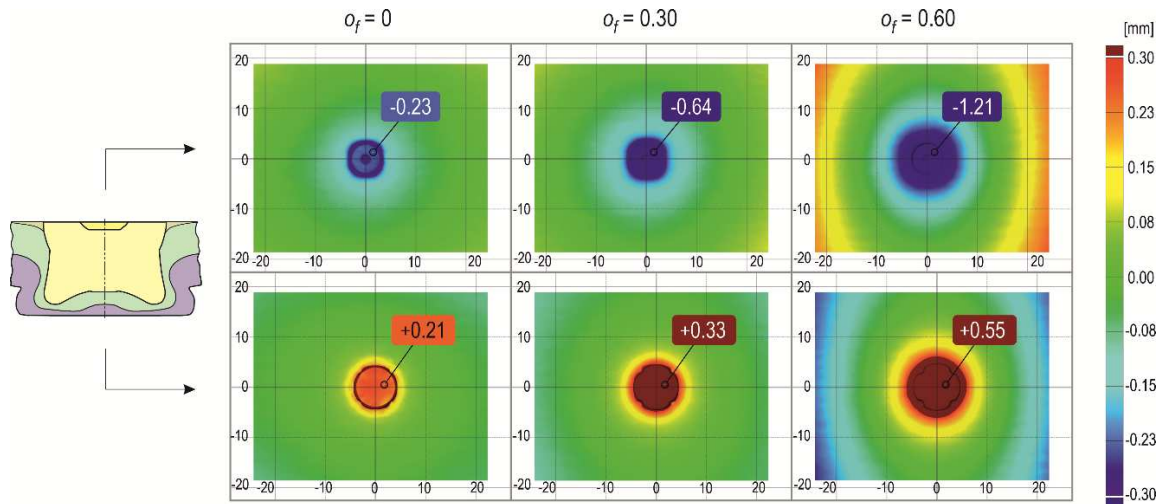


Figure 16. The influence of the offset value (o_f) on the sheet deformation in the joint axis area ($h_d=1.45$ [mm]).

The presented distributions of deviations on the sheets result from the fact that a rivet is pressed into the sheets. The sheets are pressed into the die cavity. The higher the offset values, the greater the deviations from the base plane of the sheets. In the case of deformation of the upper and lower sheets, the deviations in the position of the external surfaces varied from positive to negative values. During the forming process, the offset value was controlled with an accuracy of 0.01 [mm]. After forming the joint and withdrawing the tools, the existing stresses in the deformed sample elements caused them to relax (Figure 17). The total deviations in the finished joint around the joint were a superposition of the deviations resulting from the phenomenon of material relaxation and the deformation resulting from the pressing of the rivet into the sheets. The existing stresses caused relaxation of the surfaces of the joined elements. As a result, the values of deviations from the nominal model changed: for the sheets from their initial position, for the front surface of the rivet and the outer surface of the embossment from the position set by the forming tools. In the case of the connection for $o_f=0$ [mm], the rivet face was below the reference plane by 0.23 [mm]. For the joint with $o_f=0.3$ [mm], the rivet face was below the reference plane by 0.64 [mm]. And in the case of the joint for $o_f=0.6$ [mm], the rivet face was below the reference plane by 1.21 [mm]. The difference between the offset value in the forming process and the measured position of the rivet face (relative to the base plane) is the value of the spring back value of the joined sheets. Examples of the total deviation of the planes of the joined sheets from their base position are shown on the 3D scan model of the "CR" joint (Figure 18). In each of the cases presented in Figure 18, the nominal value of the distance between the upper and lower surfaces of the joint should be 4.45 [mm]. The higher the offset value, the greater the difference between the upper and lower surfaces distances. Deformations of the joined elements around the joint are extremely important when joining thin-walled elements together. It is required to maintain the assumed nominal parameters of the shape and dimensions of the part. The method of predicting the surface deviation of joined aluminum alloy elements using "SPR" is presented in [45]. During the tests, the influence of the rivet height on the joining process and the deformation of aluminum alloy sheets was analysed.

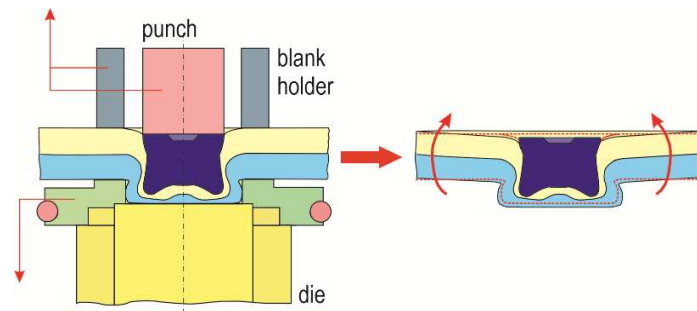


Figure 17. The schematics of: a) the blank holder acting during formation process, b) the effect of the sheet material relaxation after the tools were withdrawn.

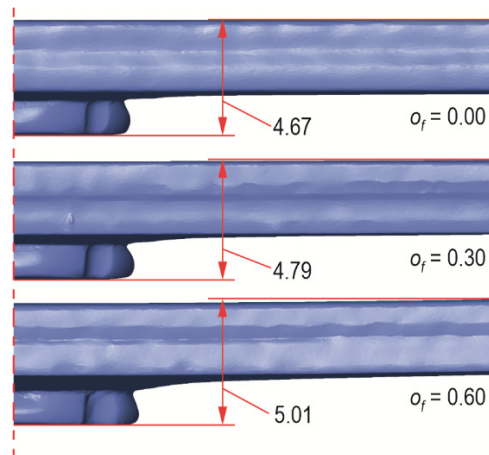


Figure 18. The examples of the influence of the offset value (o_f) on the sheet deviations – $h_d=1.45$ [mm].

3.3. Strength and failure mechanism of the CR joint

A certain regularity was observed for all joint variants - the smaller the depth of the die, the greater the maximum shear force of the lap joint (Figure 19). For each variant of the joint formed using a die of three different depths, an increase in shear force was obtained as the offset value increased. The use of a die ($o_f=0$ [mm]) with a greater depth than $h_d=1.45$ [mm], e.g. $h_d=1.60$ [mm], resulted in a reduction in the maximum load capacity of the joint in the shear test by 2.5%, and for $h_d=1.75$ [mm] it reduced the maximum average shear force of the joint by 3.5%. The forming force for $o_f=0$ [mm] was reduced by increasing the die depth from 1.45 [mm] to 1.75 [mm] by 12% (Figure 9, 10). Instead of increasing the size of the additional rivet, the strength of the clinch joint can be increased by local thermal heating by resistance welding [7,46]. However, this requires a special stand and modified tools. This method of increasing the load capacity of the joints causes thermal changes in the structure of the material.

Examples of shear force-displacement diagrams for a series of 5 samples of joints formed with different die depth $h_d=1.45$, 1.60 and 1.75 [mm] and offset $o_f=0$ [mm] are presented in Figure 20. The course of the shear force-displacement diagrams was very similar, but the maximum joint shear force was different. In the initial phase of loading the joint, the curves had slightly different angles of the linear section. Therefore, it was decided to compare the curves of the average shear force-displacement diagrams and the stiffness-displacement diagrams of the "CR" joint (Figure 21).

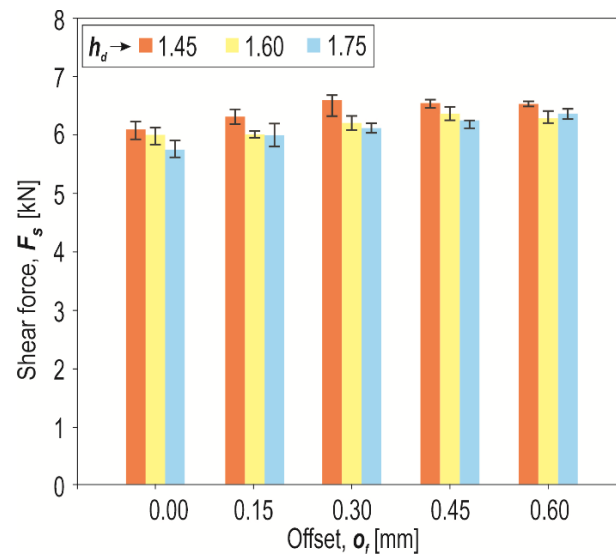


Figure 19. The influence of the depth of the die (h_d) and the offset value (o_f) on the maximum shear force during tensile shear tests of the “CR” joint.

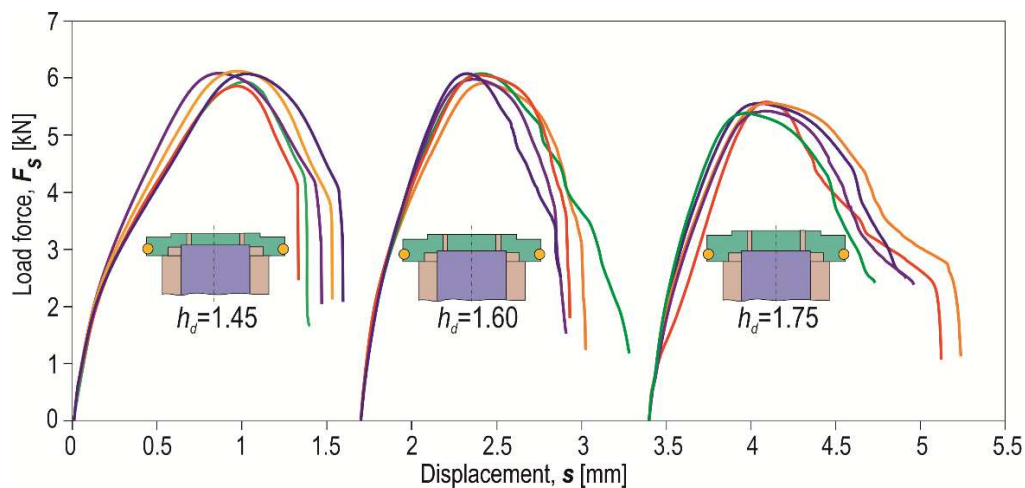


Figure 20. The examples of the forming force-displacement diagrams for “CR” joint formed with the different values of the depth of the die (h_d in [mm]) and offset value $o_f=0$ [mm].

The use of an additional rivet can be used to strengthen or repair a damaged clinch joint [24]. The authors showed that increasing the pressing force of a special tubular rivet resulted in an increase in the size of the interlock and the load capacity of the joint. In addition to the maximum load capacity of the pressed joints, the aspect of joint stiffness is extremely important. One of the works that includes research on joint stiffness [47]. The authors analysed the load parameters and joint stiffness for a combination of aluminum alloy and copper alloy materials. These are low-strength materials. HX340 steel sheets are a group of materials with increased strength that are increasingly used in car bodies [48].

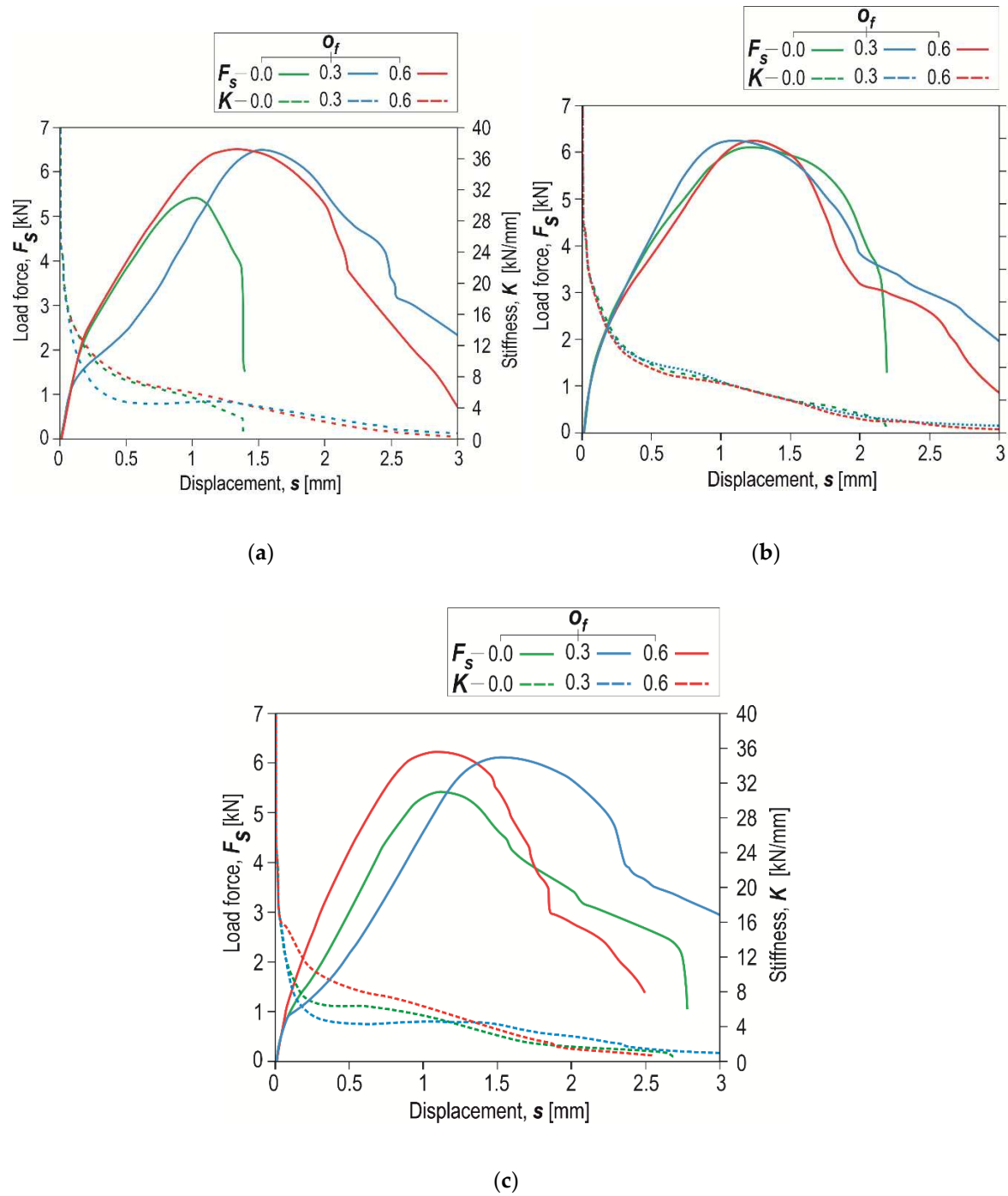


Figure 21. The examples of the forming force-displacement diagrams and stiffness-displacement diagrams for “CR” joint formed with the depth of the die h_d : a) 1.45 [mm], b) 1.60 [mm], c) 1.75 [mm].

To analyse the influence of the depth of the die (for a constant offset value) on the change in joint stiffness, the calculated joint stiffness values for three values of $h_d=1.45$, 1.60 and 1.75 [mm] are presented (Figure 22a). The joint made using a die with $h_d=1.60$ [mm] was characterized by the highest stiffness. Increasing the depth of the die from 1.45 [mm] to 1.6 [mm] resulted in an increase in stiffness. For joints made using a die of $h_d=1.75$ [mm], a decrease in joint stiffness was observed. In each of the analysed cases the highest joint stiffness was obtained from the offset value $o_f=0$, 0.3 and 0.6 [mm] to the displacement amount of 0.2 [mm] (Figure 22). When the offset value $o_f=0.3$ [mm] was used, the difference in stiffness increased as the displacement increased (Figure 22b). For the highest

offset value $o_f=0.6$ [mm], the differences between stiffnesses for joints formed using a die of different depth were the smallest (Figure 22c).

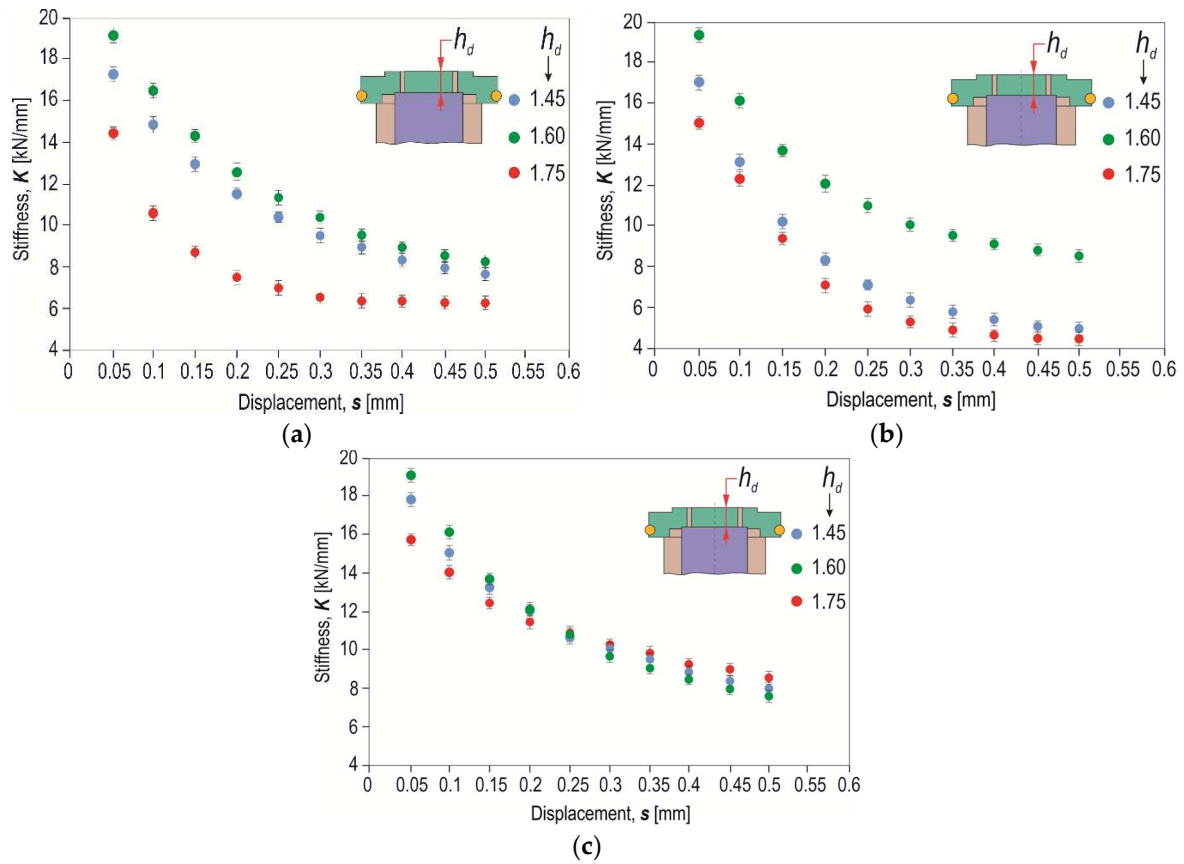


Figure 22. The influence of the depth of the die (h_d) on the joint stiffness for different values of displacement for offsets o_f : a) 0 [mm], b) 0.3 [mm], c) 0.6 [mm].

When carrying the load in the joint, there is a specific system of forces acting on the internal surfaces of the joint. These forces create a torque moment that causes the rivet to rotate in the joint. As the load increases, the sheets bend and the rivet is pulled out of the lower sheet (Figure 23). Figure 23 shows an example of the behaviour of the joint elements during a shear test of a lap joint of 1.5 [mm] thick sheets made of HX340 steel.

When joining, for example, aluminium alloys, smaller deformations of the sheets are observed during the shear test [49]. The authors presented the possibility of the two-stage formation of a clinch joint with an additional deformable rivet. Unfortunately, such a process is more complex, time-consuming, and more expensive than conventional clinch-rivet joining process.

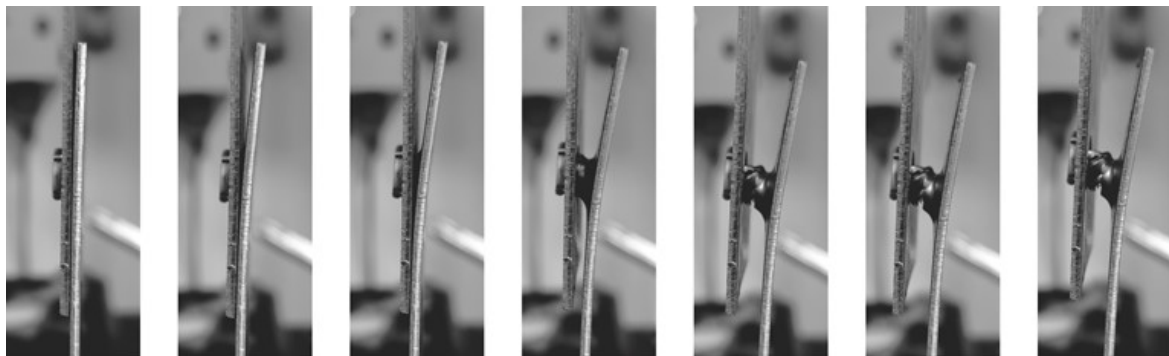


Figure 23. The example of the samples deformation stages during tensile shear test.

Although the plane of action of the force loading the lap joint was in the common plane of the sheets during the shear test, the sheets were bent. During the shear test of a lap joint, there is a certain system of forces relative to the plane of load action (Figure 24). Part of the height of the rivet (h_b) relative to the common surface of the sheets is greater in the lower sheet (Figure 24). The rivet is more blocked on the lower sheet and creates resistance so that it causes a greater bending of the upper sheet (in Figure 23 - right sheet). Forces F_1 and F_2 act on the joint in one plane. The embossment surfaces of the sheets that carry the load are not uniformly located in relation to the line of load action. The force F_2' acts on the distance h_b relative to the line of action of the load forces:

$$M_2 = F_2' \cdot e_1. \quad (1)$$

The force F_1 is distributed on the surfaces that is below and above the line of action of the load forces:

$$\begin{aligned} -M_{1.3} &= F_{1.3}' \cdot e_4, \\ -M_{1.2} &= F_{1.2}' \cdot e_3, \\ M_{1.1} &= F_{1.1}' \cdot e_2. \end{aligned} \quad (2)$$

Forces acting in the tensile shear test:

$$F_1 = F_{1.1}' + F_{1.2}' + F_{1.3}', \quad (3)$$

$$F_2 = F_2'. \quad (4)$$

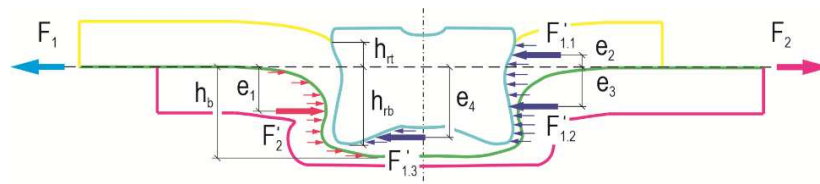


Figure 24. The forces acting scheme during the tensile shear test of the “CR” joint.

The greater the depth of the die (h_d), the greater the reaction moment of internal forces in the joint and the bending of the sheet on the side of the rivet press-in (Figure 25). In the case of using a die with a depth of $h_d=1.45$ [mm], the greater the offset used, the greater the bending of the sheet metal was observed. The rivet was pressed deeper and blocked more tightly. Increasing the depth of the die caused the rivet to be pressed deeper into the materials being joined. The higher the depth of the die, the greater the bending of the sheet metal (for the case of offset value $o_f=0$ [mm]). The higher the offset value, the smaller the bending was observed for joints formed with a depth greater than $h_d=1.45$, i.e. 1.60, or 1.75 [mm].

To discuss the differences in the behaviour of the rivet in the tensile shear test, the results of some cases of joint formation have been presented. For all joint combinations tested, two failure mechanisms occurred during the tensile shear test of the “CR” lap joint (Figure 26). The first and most common is the splitting of the embossment of the upper and lower sheets. The rivet remained in the upper plate, with the embossment partially failure. The embossment of the top sheet was failure. The second failure mechanism occurred for the highest offset value and the depth of the die. Part of the embossment of the upper sheet was failure and remained in the lower sheet. The greater the offset used, the more the rivet axis was deflected in the lap joint shear test. In the case of joints formed using a die with $h_d=1.45$ [mm], it was observed that the higher the offset value of the joint, the greater the deflected rivet axis during the tensile shear test of the lap joint. However, for joints formed with a constant value o_f and a variable value of h_d , during the tensile shear test it was observed that the deflection of the rivet axis decreased when the higher the value of the depth of the die.

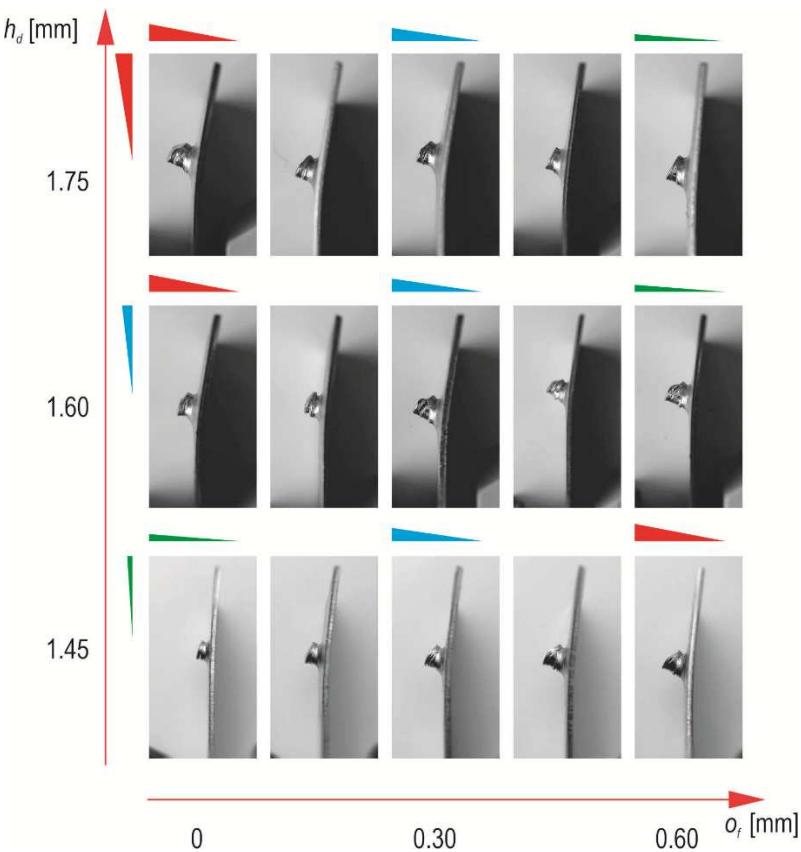


Figure 25. The influence of the depth of the die (h_d) and the offset value (o_f) on the deviations of the sheets after tensile shear test.

For the case of the formed joint (for $h_d=1.6$ [mm], and $o_f=0$ [mm]) in the tensile shear test, it was not possible to determine the deviation of the rivet axis (the rivet was not exposed from the upper sheet).

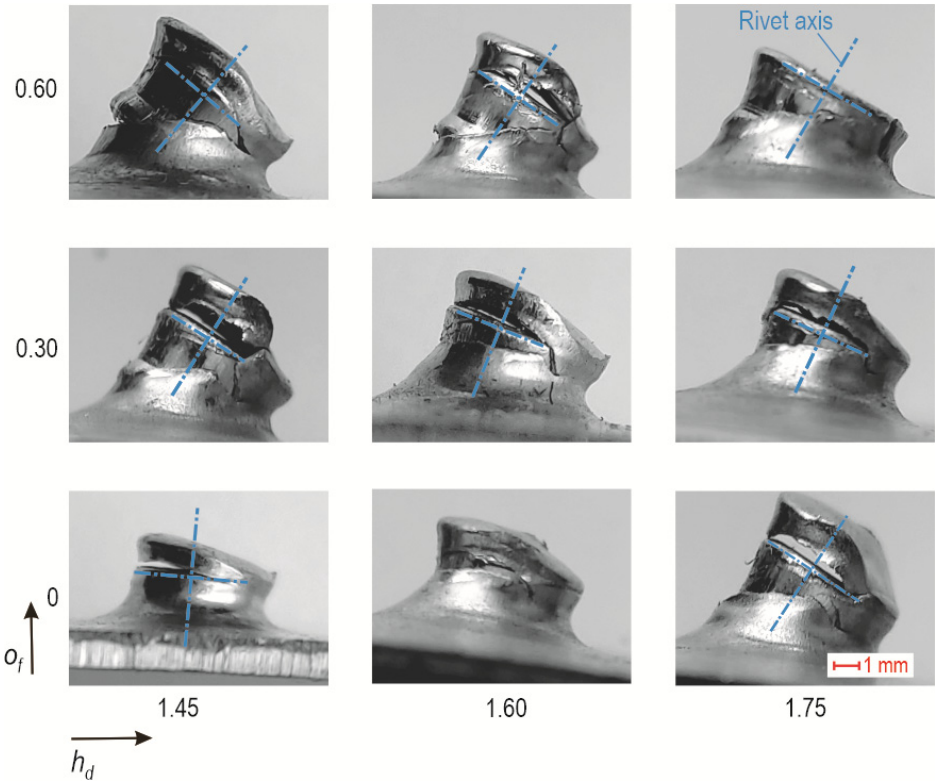


Figure 26. The macrostructure of the “CR” joint after tensile shear with a marked deviation of the joint axis.

4. Conclusions

The presented research shows the influence of the use of different rivet insertion depths on the strength of the joint formed using a die of different depths $h_d=1.45, 1.60$ and 1.75 [mm]. It is possible to strengthen the “CR” joint by changing the depth of pressing the steel rivet without disturbing the cohesion of the sheet material. However, the use of a higher rivet press value resulted in a significant increase in forming force and energy consumption. Significant and most important information obtained from the conducted research:

- As the depth of the die (h_d) increased, the maximum value of the forming force decreased. The relation was observed for each of the analysed offset values. Increasing the depth of insertion of the rivet (o_f) results in an increase in the force required to form the joint.
- The smaller the die depth (h_d) used, the greater the maximum shear force obtained in the lap joint. The load capacity of the “CR” joint was increased by increasing the offset value (o_f). However, using a larger offset required greater forming force, and the process was more energy consuming.
- For all analysed cases of using the depth of the die (h_d), there was a relation that with an increase in the insertion depth o_f , both the external height of the embossment and the largest rivet diameter d_i increased. Joints made using a die with a depth of $h_d=1.45$ [mm] were characterized by the largest embossment dimensions.
- The higher the value of the rivet offset (o_f), the more the rivet flows plastically in the direction transverse to the movement of the punch. The deeper the die used, the radial flow of the rivet in its lower part decreased and the flow increased in the direction consistent with the displacement of the punch. For all three die depths $h_d=1.45, 1.60$ and 1.75 [mm], the value of the interlock parameter increased with the increase of the offset value (o_f). The maximum value of the parameter t_u characterized joints made with $h_d=1.60$ [mm] and $o_f=0.60$ [mm].
- Up to the displacement range of ≈ 0.2 [mm], the highest stiffness was obtained for joints formed with a depth of the die $h_d=1.60$ [mm]. Despite increasing the depth of the die to 1.75 [mm] (the rivet is pressed deeper in the joined material), greater joint stiffness was not achieved. In only one case in the range s from 0.3 to 0.5 [mm], for joints formed with a die of $h_d=1.75$ [mm] depth, the stiffness of the joints was the highest.
- The analysis of the deformation of the sheet metal surface in the area of the joint showed that for each value of the o_f , the upper plane of the rivet in the joint is below the given value (measured in relation to the nominal model). As the offset increases, the deformation of the sheets and the position of the upper surface of the rivet changes. The highest deviations of the sheets occurred for a formed joint with $o_f=0.6$ [mm] and with a depth of the die $h_d=1.45$ [mm].

Author Contributions: Conceptualization, Ł.B., J.M. and W.W.; methodology, Ł.B., J.M. and W.W.; software, W.W.; validation, Ł.B., W.W.; formal analysis, J.M.; investigation, Ł.B., J.M. and W.W.; resources, J.M.; data curation, Ł.B.; writing—original draft preparation, J.M.; writing—review and editing, Ł. B., W.W.; visualization, Ł.B., J.M. and W.W.; supervision, J.M.; project administration, Ł.B.; funding acquisition, Ł.B., J.M. and W.W. All authors have read and agreed to the published version of the manuscript.

Funding: This research received no external funding.

Institutional Review Board Statement: Not applicable.

Informed Consent Statement: Not applicable.

Data Availability Statement: The research data can be obtained from the authors.

Conflicts of Interest: The authors declare no conflicts of interest.

References

1. Heeren, R.; Timmermann, R. Mechanical Joining in the Automotive Industry. **2002**, SMWC X, Paper No. 4-1.
2. Zhou, Y.; Lan, F.; Chen, J. Influence of tooling geometric parameters on clinching joint properties for steel-aluminum car-body structures. In Proceedings of 3rd IEEE International Conference on Computer Science and Information Technology, ICCSIT; Chengdu, IEEE, China, 7-10 July 2010.
3. Mucha, J.; Witkowski, W. The experimental analysis of the double joint type change effect on the joint destruction process in uniaxial shearing test. *Thin-Wall. Struct.* **2013**, *66*, 39–49.
4. Saberi, S.; Enzinger, N.; Vallant, R.; et al. Influence of plastic anisotropy on the mechanical behavior of clinched joint of different coated thin steel sheets. *Int. J. Mater. Form.* **2008**, *1*, 273–276.
5. Mucha, J.; Kaščák, L.; Spišák, E. Joining the car-body sheets using clinching process with various thickness and mechanical property arrangements. *Arch. Civ. Mech. Eng.* **2011**, *1*, 135–148.
6. Zhang, X.; Chen, C.; Peng, H. Recent development of clinching tools and machines. *Int. J. Adv. Manuf. Technol.* **2022**, *121*, 2867–2899.
7. Džupon, M.; Kaščák, L.; Cmorej, D.; Čiripová, L.; Mucha, J.; Spišák, E. Clinching of high-strength steel sheets with local preheating. *Appl. Sci.* **2023**, *13*, 7790.
8. Zhang, Y.; Wang, C.; Shan, H.; Li, Y.; Luo, Z. High-toughness joining of aluminum alloy 5754 and DQSK steel using hybrid clinching–welding process. *J. Mater. Process. Technol.* **2018**, *259*, 33–44.
9. Lee, C.-J.; Shen, G.; Kim, B.-M.; Lambiase, F.; Ko, D.-C. Analysis of failure-mode dependent joint strength in hole clinching from the aspects of geometrical interlocking parameters. *Metals*, **2018**, *8*, 1020.
10. He, X.; Pearson, I.; Young, K. Self-pierce riveting for sheet materials: state of the art. *J. Mater. Process. Technol.* **2008**, *199*, 27–36.
11. Ang, H.Q. An overview of self-piercing riveting process with focus on joint failures, Corrosion issues and optimisation techniques. *Chin. J. Mech. Eng.* **2021**, *34*, 1–25.
12. Xing, B.; He, X.; Zeng, K.; et al. Mechanical properties of self-piercing riveted joints in aluminum alloy 5052. *Int. J. Adv. Manuf. Technol.* **2014**, *75*, 351–361.
13. Zhang, X.; He, X.; Gu, F.; Ball, A. Self-piercing riveting of aluminium–lithium alloy sheet materials. *J. Mater. Process. Technol.* **2019**, *268*, 192–200.
14. Zhao, L.; He, X.; Xing, B.; Zhang, X.; Cheng, Q.; Gu, F.; Ball, A. Fretting behavior of self-piercing riveted joints in titanium sheet materials. *J. Mater. Process. Technol.* **2017**, *249*, 246–254.
15. He, X.; Wang, Y.; Lu, Y.; et al. Self-piercing riveting of similar and dissimilar titanium sheet materials. *Int. J. Adv. Manuf. Technol.* **2015**, *80*, 2105–2115.
16. <https://global.abb> (30.11.2023).
17. Heyser, P.; Wiesenmayer, S.; Frey, P.; et al. Consideration of the manufacturing history of sheet metal components for the adaptation of a clinching process. *Proc. Inst. Mech. Eng. L: J. Mater.: Des. Appl.* **2022**, *236*, 1203–1215.
18. Chen, C.; Zhang, X.; Wen, C.; Yin, Y. Effect of blank holder force on joining quality of the flat clinch-rivet process. *Int. J. Adv. Manuf. Technol.* **2022**, *121*, 6315–6323.
19. Kaščák, L.; Spišák, E.; Mucha, J. Evaluation of properties of joints made by clinching and self-piercing riveting methods. *Acta Metall. Slovaca*. **2012**, *18*, 172–180.
20. Mucha, J.; Boda, L.; Poręba, M.; Witkowski, W. Mixed-mode loading tests for determining the mechanical properties of clinched joints with an additional rivet used in the assembly of thin-walled structures. *Thin-Wall. Struct.* **2023**, *190*, 110965.
21. Chen, C.; Li, Y.; Zhang, H.; Li, Y.; Pan, Q.; Han, X. Investigation of a renovating process for failure clinched joint to join thin-walled structures. *Thin-Wall. Struct.* **2020**, *151*, 106686.
22. Chen, C.; Ran, X.; Pan, Q.; Zhang, H.; Yi, R.; Han, X. Research on the mechanical properties of repaired clinched joints with different forces. *Thin-Wall. Struct.* **2020**, *152*, 106752.
23. Mucha, J.; Boda, L.; Witkowski, W. Geometrical parameters and strength of clinching joint formed with the use of an additional rivet. *Arch. Civ. Mech. Eng.* **2023**, *114*, 1–16.
24. Ren, X.; Chen, C.; Ran, X.; Li, Y.X. Zhang, Microstructure evolution of AA5052 joint failure process and mechanical performance after reconditioning with tubular rivet. *Trans. Nonferrous Met. Soc. China*. **2021**, *31*, 3380–3393.
25. Ren, X.; Chen, C.; Ran, X.; Gao, X.; Gao, Y. Investigation on lightweight performance of tubular rivet-reinforced joints for joining AA5052 sheets. *J. Braz. Soc. Mech. Sci. Eng.* **2021**, *43*, 333.
26. Chen, C.; Wu, J.; Li, H. Optimization design of cylindrical rivet in flat bottom riveting. *Thin-Wall. Struct.* **2021**, *168*, 108292.
27. Neugebauer, R.; Jesche, F.; Israel, M. Enlargement of the application range of solid punch riveting by two-piece dies. *Int. J. Mater. Form.* **2010**, *3*, 999–1002.
28. Mucha, J. The effect of material properties and joining process parameters on behavior of self-pierce riveting joints made with the solid rivet. *Mater. Des.* **2013**, *52*, 932–946.

29. Mucha, J. The numerical analysis of the effect of the joining process parameters on self-piercing riveting using the solid rivet. *Arch. Civil Mech. Eng.* **2014**, *14*, 444–454.
30. Mucha, J. The failure mechanics analysis of the solid self-piercing riveting joints. *Eng. Fail. Anal.* **2015**, *47*, 77–88.
31. Han, D.; Yang, K.; Meschut G. Mechanical joining of glass fibre reinforced polymer (GFRP) through an innovative solid self-piercing rivet. *J. Mater. Process. Technol.* **2021**, *296*, 117–182.
32. Vorderbrüggen, J.; Köhler, D.; Grüber, B.; Troschitz, J.; Gude, M.; Meschut, G. Development of a rivet geometry for solid self-piercing riveting of thermally loaded CFRP-metal joints in automotive construction. *Compos. Struct.* **2022**, *291*, 115583.
33. Eckert, A.; Neugebauer, R.; Rössinger, M.; et al. Application limits of a method to predict distortion caused by mechanical joining technologies in Car body construction. In The 8th International Conference and Workshop on Numerical Simulation of 3D Sheet Metal Forming Processes (NUMISHEET 2011), Seoul, Republic of Korea, 21–26 August.
34. Meschut, G.; Janzen, V.; Olfermann, T. Innovative and Highly Productive Joining Technologies for Multi-Material Lightweight Car Body Structures. *J. Mater. Eng. Perform.* **2014**, *23*, 1515–1523.
35. Cai W.; Lesperance, R.M.; Marin, S.P.; Meyer, W.W.; Oetjens, T.J. Digital Panel Assembly for Automotive Body-in-White. In ASME 2002 International Mechanical Engineering Congress and Exposition, New Orleans, Louisiana, USA, November 17–22, 2002.
36. EN 10143:2006. Continuously hot-dip coated steel sheet and strip - Tolerances on dimensions and shape.
37. EN 10346:2009. Continuously hot-dip coated steel flat products - Technical delivery conditions.
38. ISO 6507-1:2018. Metallic materials — Vickers hardness test — Part 1: Test method. Technical Committee ISO/TC 164, Mechanical testing of metals, Subcommittee SC 3, Hardness testing.
39. VDI/VDE 2634-3:2008-12. Optical 3D-Measuring Systems—Multiple View Systems Based on Area Scanning; Beuth Verlag GmbH: Berlin, Germany, 2008.
40. ISO 12996: 2013: Mechanical joining — Destructive testing of joints — Specimen dimensions and test procedure for tensile shear testing of single joints, Technical Committee ISO/TC 44/SC 6 Resistance welding and allied mechanical joining, (2013)
41. Kaščák, L.; Mucha, J.; Spišák, E.; et al. Wear Study of Mechanical Clinching Dies During Joining of Advanced High-Strength Steel Sheets. *Strength Mater.* **2017**, *49*, 726–73.
42. Kaščák, L.; Spišák, E.; Kubik, R.; et al. FEM Analysis of Clinching Tool Load in a Joint of Dual-Phase Steels. *Strength Mater.* **2016**, *48*, 533–539.
43. Abe, Y.; Maeda, T.; Yoshioka, D.; Mori, K.-i. Mechanical Clinching and Self-Pierce Riveting of Thin Three Sheets of 5000 Series Aluminium Alloy and 980 MPa Grade Cold Rolled Ultra-High Strength Steel. *Materials* **2020**, *13*, 4741.
44. Mori, K.; Kato, T.; Abe, Y.; Ravshanbek, Y. Plastic Joining of Ultra High Strength Steel and Aluminium Alloy Sheets by Self Piercing Rivet. *CIRP Ann.* **2006**, *55*, 283–286.
45. Tozaki, Y.; Uematsu, Y.; Tokaji, K. Effect of tool geometry on microstructure and static strength in friction stir spot welded aluminium alloys. *Int. J. Mach. Tools Manuf.* **2007**, *47*, 2230–2236.
46. Zhang, Y.; Zhang, X.; Guo, J.; Manladan, S.M.; Luo, Z.; Li, Y. Effects of local stiffness on the spot joints mechanical properties: Comparative study between resistance spot welding and resistance spot clinching joints. *J. Manuf. Process.* **2019**, *39*, 93–101.
47. He, X.; Zhao, L.; Deng, Ch.; Xing, B.; Gu, F.; Ball, A. Self-piercing riveting of similar and dissimilar metal sheets of aluminum alloy and copper alloy. *Mater. Des.* **2015**, *65*, 923–933.
48. Kaščák, L.; Cmorej, D.; Spišák, E.; Slota, J. Joining the High-Strength Steel Sheets Used in Car Body Production. *J. Adv. Sci. Technol. Res.* **2021**, *15*, 184–196.
49. Chen, C.; Zhao S.; Cui, M.; Han, X.; Fan, S. Mechanical properties of the two-steps clinched joint with a clinch-rivet. *J. Mater. Process. Technol.* **2016**, *237*, 361–370.

Disclaimer/Publisher's Note: The statements, opinions and data contained in all publications are solely those of the individual author(s) and contributor(s) and not of MDPI and/or the editor(s). MDPI and/or the editor(s) disclaim responsibility for any injury to people or property resulting from any ideas, methods, instructions or products referred to in the content.